

# Iterative FE analysis for non-invasive material modeling of a fingertip with layered structure

Mitsunori Tada\*

Noritaka Nagai†

Hiroaki Yoshida‡

Takashi Maeno§

\*‡ Digital Human Research Center, National Institute of Advanced Industrial Science and Technology (AIST)

\*‡ CREST, Japan Science and Technology Agency (JST)

† School of Integrated Design Engineering, Graduate School of Science and Technology, Keio University

§ Department of Mechanical Engineering, Keio University

## ABSTRACT

We propose a method to estimate material constants of living soft tissue. It allows modeling of non-linear material properties of soft tissue even for subsurface layer in non-invasive manner. It employs medical imaging modality and iterative finite element (FE) analysis. The iterative FE analysis determines material constants so that the error between measured MR volume data and synthesized MR volume data is minimized. The synthesized MR volume data is obtained by transforming the pre-compression MR volume according to the displacement field computed by FE analysis. The proposed method was applied to a silicon rubber phantom and an index finger of male subject. The former showed good performance of our method that estimated material constants with the accuracy of 7%. The latter revealed an essential feature of a fingertip: the cortical layer is more rigid than the inner layer that is consistent with the previous researches.

**Keywords:** soft tissue, material constant, Ogden model, iterative FE analysis, MRI

## 1 INTRODUCTION

Neural impulses emitted from the tactile receptors evoke the sense of touch. In order to gain quantitative understandings in the mechanism of touch, it is fundamental to understand the subsurface mechanical behavior of a fingertip in contact with an object, since the mechanical stimulus is the main trigger for the emission of the neural impulses. Mechanical characterization of a fingertip is therefore one of the key elemental technology in the studies of haptics.

Pawluk and Howe investigated dynamic lumped element response of the human finger pad [1]. A quasi-linear visco-elastic model was employed that successfully explained the reaction force against dynamic indentation with a flat probe. They also investigated dynamic, distributed pressure response [2] under the same conditions. A modified contact model of a rigid plane and a linear visco-elastic sphere was introduced to explain the feature of the distributed pressure response. On the contrary, Nakazawa et al. characterized impedance of a finger pad under step and ramp shearing force [3]. The Kelvin model was employed to explain the dynamic characteristics of finger pad. They concluded that the stiffness in the shearing direction changes depending on the finger, applied normal force, and the direction of the shearing force. These researches have tried to model the mechanical behavior of finger pad from a

macroscopic point of view; i.e. they assumed that the finger pad is represented as a mass-spring-dumper system. They are not thus appropriate for the precise modeling of the subsurface mechanical behavior.

The rapid progress in computational power allows us to conduct finite element (FE) analysis of massive mechanical structures. This technique is being applied to the studies of haptics, because of its ability to simulate and predict subcutaneous mechanical behaviors [4, 5, 6]. In these researches, fingertips have multi-layered structure represented as a set of finites elements. Precise material characterization of each layer is crucial for the realistic simulation of the mechanical behaviors.

Maeno et al. constructed a cross-sectional finger model with three layers: epidermis, dermis and subcutaneous tissue. All the three layers were assumed to be linear elastic and isotropic medium with different material constant determined from a cadaver tissue [4]. Therefore, it is difficult to take individual differences into their model.

Dandekar et. al created three-dimensional FE models of primate fingertips with five layers: epidermis, dermis, adipose tissue, fibrous matrix and bone [6]. Same as Maeno's model, all the soft tissue were assumed to be linear elastic and isotropic medium. They performed forward FE analyses and compute the surface deflection under line loadings, changing the ratio of elastic moduli by a factor of 10. The optimal ratio of the elastic moduli was determined so that the error between the measured deflection and the computed surface deflection is small enough. The absolute values of the elastic moduli are then obtained by adapting the computed force-displacement relationships to that obtained by experiments. Though their models have capability to conduct subject-specific analysis, it is limited to the range of small deformation, since the surface deflection was at most 1.0 mm in their analysis.

We intend to conduct finite element analysis for three-dimensional fingertips both for haptics study and for product design. At least dozens of subject-specific FE models with precise subcutaneous geometries and material properties are required to compute the mechanical behavior of fingertips. In this paper, we propose a method to estimate material constants of living soft tissue. This method allows non-invasive and non-linear material modeling even for layered structure, since it employs medical imaging modality and iterative FE analysis.

## 2 METHOD

### 2.1 MRI Based Elastographies in the Literature

Recent progress in diagnostic imaging modalities allows us to develop new elasticity imaging techniques. Magnetic resonance elastography (MRE) is one of the promising method [7]. It visualizes strain waves that propagate within soft tissue by using MRI. We can estimate distribution of the stiffness even for subsurface tissue, since the wavelength visualized by MRE is proportional to the

\*e-mail: m.tada@aist.go.jp

†e-mail: y09677@educ.cc.keio.ac.jp

‡e-mail: hiro-yoshida@aist.go.jp

§e-mail: maeno@mech.keio.ac.jp

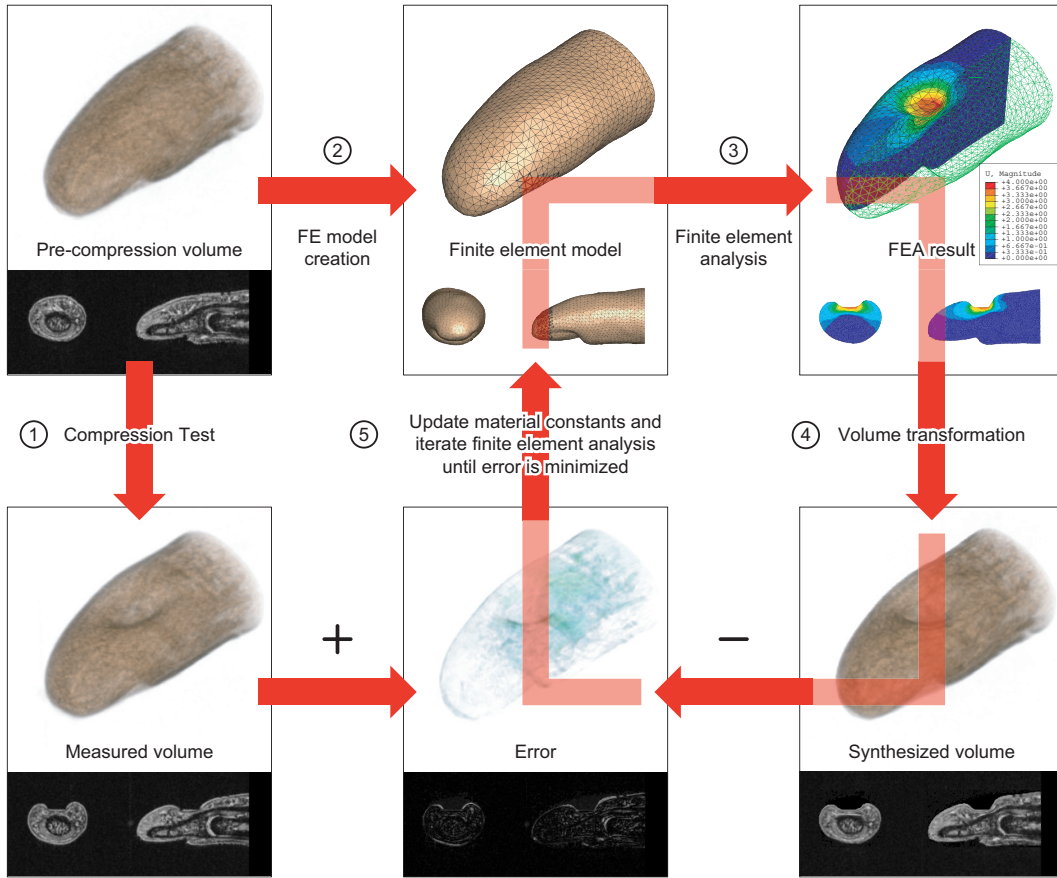


Figure 1: Overview of the iterative FE analysis.

stiffness. However, damping and reflection of the strain waves that induce fatal estimation error are not negligible when applying this technique to actual fingertip.

Quasi-static MRE is another elasticity imaging method [8]. It employs a discrete constitutive equation of linear elasticity to reconstruct the stiffness distribution from the strain image visualized by MRI. It was found, however, that in this method, since the constitutive equation assumes small deformation, we can not consider non-linear characteristics of fingertip.

## 2.2 Proposed Method – Iterative FE Analysis

In order to compute deformation of fingertip under arbitrary loading conditions, we have to take subcutaneous structures as well as non-linear material characteristics of soft tissue into considerations. The estimation method of material constants presented in this study accounts for these requirements. Shown in Figure 1 is the overview of the proposed method. It is divided into following three procedures.

**MR Compression Test** Compress the fingertip inside MRI in order to visualize three-dimensional deformation of the subcutaneous structure, as shown in ① of Figure 1. The compression force is measured by using MR compatible force sensor [9], at the same time. Let us call the obtained volume data of the compressed fingertip as measured volume.

**FE Model Generation** Generate a subject-specific FE model with precise subcutaneous geometries from the pre-compression

MR volume data as shown in ② of Figure 1. The same boundary conditions as the MR compression test are assigned to this FE model. The material constant of each anatomical part is initialized to reasonable value.

**Iterative FE Analysis** Compute the deformation of the FE model under given conditions as shown in ③ of Figure 1, and transform the pre-compression MR volume according to the computed displacement field as shown in ④ of Figure 1. Let us call the transformed MR volume data as synthesized volume.

Then update the material constants so that the error between the measured volume and the synthesized volume is decreased, and iterate these procedures (⑤, ③ and ④ of Figure 1) until the error is minimized. The resultant material constants are the final estimates.

This method has remarkable advantages over the other MRI based elastographies described in Section 2.1. Firstly, it allows estimation of material constants taking large deformation and non-linear material properties into consideration even for the subsurface tissue. This is because of the medical imaging modality and FE analysis employed in this method. MRI allows us to observe deformation of subsurface tissue directly, while FE analysis allows us to introduce complicated mechanics of soft tissue such as large deformation, non-linear material properties and contact problem into the estimation.

Secondly, since the material constants are determined so that the error between the measured volume and the synthesized volume is

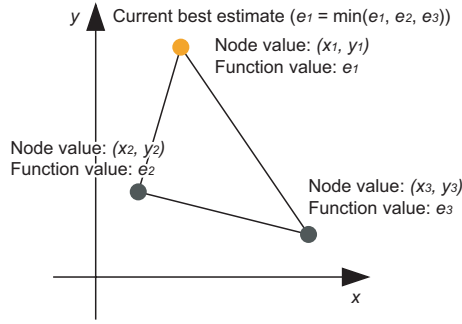


Figure 2: Schematic illustration of two-dimensional simplex.

minimized, the reproducibility of FE analysis where the estimated material constants are assigned is maximized.

Finally and equally important for numerical simulation such as FE analysis, errors in computed deformation are evaluated in detail by comparing a measured volume and a synthesized volume. Accuracy of FE analysis is typically evaluated by relation between indentation depth and resultant reaction force, although deformation and other mechanical quantities such as stress/strain are computed for every node. Different from such local evaluation, this method allows us to evaluate entire deformed profile of soft tissue; i.e. it enables global evaluation.

### 2.3 Implementation Details

This section describes implementation details of the iterative FE analysis.

We employed normalized mutual information [10] (NMI) and sum of squared differences [11] (SSD) for similarity measure of two volumes. The NMI is effective for the comparison of two volumes with different intensity pattern, while the SSD is effective for that with similar intensity pattern. We used either of them depending on the quality of the obtained MR volume. The optimization of the iterative FE analysis is thus amounts to a problem of finding the maximum of NMI or minimal of SSD between a measured volume and a synthesized volume.

Downhill simplex method [12] is employed for the optimization of the similarity measure. It is a numerical optimization technique widely used in a problem that has non-smooth evaluation function or has difficulty in the direct computation of the derived function. This optimization method is appropriate for the iterative FE analysis, since analytical computation of the derived function is difficult in general.

Figure 2 shows a schematic illustration of two-dimensional simplex. This method has two termination criteria: (1) diameter of the simplex and (2) difference of the function value. The optimization is iterated until the first criterion is less than  $tolx$  and the second criterion is less than  $tolf$ . By using notations in Figure 2, the former and the latter is described as Equation (1) and Equation (2), respectively.

$$tole = \max(\text{abs}(x_2 - x_1), \text{abs}(x_3 - x_1), \text{abs}(y_2 - y_1), \text{abs}(y_3 - y_1)) \quad (1)$$

$$tolf = \max(\text{abs}(e_2 - e_1), \text{abs}(e_3 - e_1)) \quad (2)$$

The iterative FE analysis was implemented using a general-purpose non-linear FE analysis program ABAQUS (ABAQUS, Inc.) and a high-level program language MATLAB (The MathWorks, Inc.). Forward FE analysis is performed using ABAQUS,

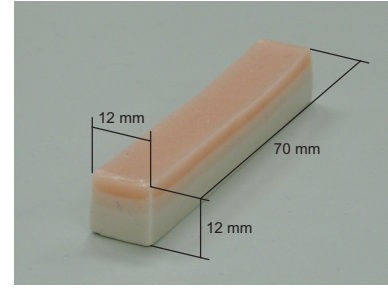


Figure 3: Silicon rubber phantom with three layers.

while the other processes, volume transformation, computation of volume similarity, and optimization of volume similarity is performed using MATLAB.

## 3 EXPERIMENTAL FOR A SILICON RUBBER PHANTOM

### 3.1 MR Compression Test

We conducted iterative FE analysis for a three-layered silicon rubber phantom. Since the material property of each layer was identified by a separate uni-axial compression test, we can evaluate the accuracy of the iterative FE analysis. Figure 3 shows the silicon rubber phantom with the dimension of  $12 \times 12 \times 70$  mm. It has the same three-layered structure along the longitudinal direction. Mechanical behavior of the center cross section of this phantom is represented by a plane strain model, if the boundary conditions are also identical along this direction. We imaged two-dimensional center cross section slice instead of three-dimensional data for this reason.

This phantom was glued to a base plate that was inserted into a small saddle coil placed at the center of a 4.7 T, 230 mm bore MRI scanner (Unity INOVA, Varian, Inc.). The high magnetic field of this scanner ensured high signal-to-noise ratio of the obtained data. The image data was obtained with a spin echo multi slice sequence (SEMS) with TR/TE of 500/19 msec, whose field of view (FOV) was  $25 \times 25$  mm and image size was  $256 \times 256$  pixel. Resolution of the image data was thus  $0.998 \mu\text{m}/\text{pixel}$ . It took about 12 minutes to obtain one slice.

A mechanical compressor and an MR-compatible force sensor [9] were employed for the compression test. Both are highly MR-compatible: completely free from magnetic materials and electric circuits. A flat indenter was glued to the top surface of the phantom and was indented in 7 steps. The maximum indentation depth was about 3.5 mm. Compression force was measured with the frequency of 0.1 Hz during the imaging process.

Figure 5 (a) shows the MR images of the center cross section of every two steps during the compression test. A three-layered structure of this phantom is clearly imaged. Let us call each layer as first, second and third layer respectively from the top for convenience of following explanation. Observed compression force and its standard deviation are also shown in the top left of each panel.

### 3.2 FE model generation

An FE model of the center cross section of the phantom was prepared for iterative FE analysis. Figure 4 (a) shows the generated FE model. This model was manually created by extracting boundaries from a pre-compression MR image. It is composed of second-order quadrilateral elements. The total number of elements and nodes was 36 and 133, respectively.

Same as the MR compression test, bottom surface was pinned while the top surface was configured to glue to the indenter (rough

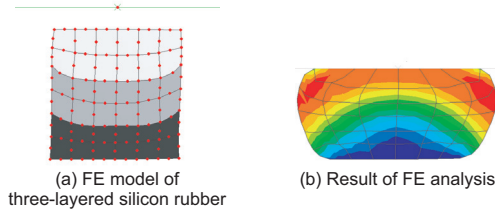


Figure 4: Generated finite element model of the silicon rubber phantom and result of finite element analysis.

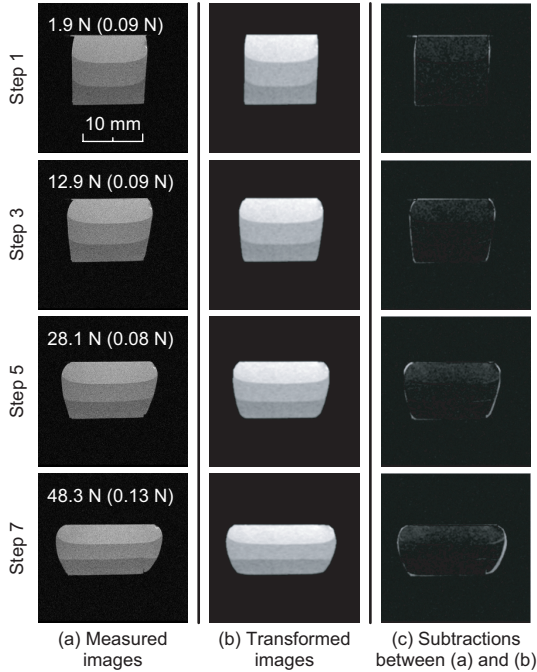


Figure 5: Measured images, synthesized images and subtractions between these images for different indentation depth.

contact in ABAQUS).

To deal with non-linear material property of silicon rubber, first-term Ogden model was employed [13]. It is a hyper-elastic model widely used in the analysis of rubber-like material and soft tissue [5]. This model has two material constants,  $\mu$  and  $\alpha$ . The latter was fixed to 1.4 in order to ensure the uniqueness of  $\alpha$  (see [14] and Section 3 of [15] for detail). Each layer has, therefore, one material constant  $\mu$  to be estimated. Let us call the material constant of each layer as  $\mu_{1st}$ ,  $\mu_{2nd}$  and  $\mu_{3rd}$ , respectively.

Figure 4 (b) shows the result of the FE analysis for this model in which the true material constants identified by a separate uni-axial compression test are assigned.

### 3.3 Iterative FE Analysis

The iterative FE analysis was performed in two steps, coarse to fine manner. In the first step, we applied constraint to the three material constants that they are equal; i.e.  $\mu_{1st} = \mu_{2nd} = \mu_{3rd}$ . First row of Table 1 shows the initial values for this estimation. In the next step of the iterative FE analysis, the material constants are assumed to be independent. In this step, the initial value of each material

Table 1: Initial material constants, estimated material constants and their estimation error.

	$\mu_{1st}$	$\mu_{2nd}$	$\mu_{3rd}$
Initial values (MPa)	1.00e-1	1.00e-1	1.00e-1
Estimated values (MPa)	2.01e-2	3.35e-2	6.32e-2
Identified values (MPa)	2.11e-2	3.57e-2	6.56e-2
Error (%)	4.73	6.16	3.66

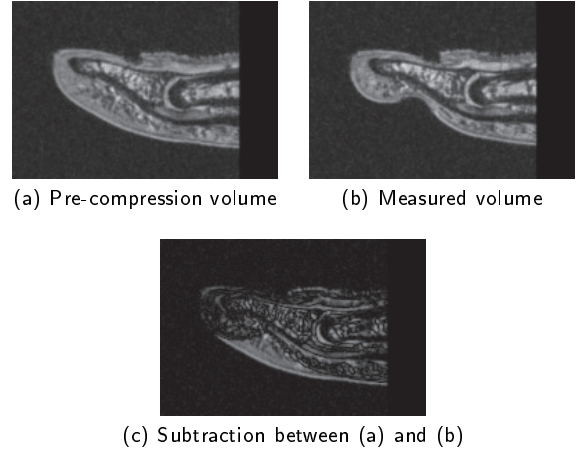


Figure 6: Subtractions between the pre-compression MR volume and the measured MR volume.

constant was set to the estimated result in the first step.

We chose to employ NMI as similarity measure of each optimization. The images captured in step 1, 3, 5 and 7 were used to compute the NMI. In the first step,  $tolx$  was 1.00e-3 MPa and  $tolf$  was 1.00e-3, while in the second step,  $tolx$  was 1.00e-5 MPa and  $tolf$  was 1.00e-5. Our current implementation requires approximately 18 minutes (6 iterations in the first step and 22 iteration in the second step) using a Windows machine of Pentium M 1.3 GHz with memory of 768 MB.

Figure 5 shows the result of the iterative FE analysis in the second step. Each panel shows the measured images, synthesized images in the final iteration, and subtractions between these two images, respectively. One can observe good correspondence of all the profile including the boundary between the layers. The second row of Table 1 shows the estimated material constants for this silicon rubber phantom, while the third row shows the identified material constants for a standard test piece of each silicon rubber. The fourth row of Table 1 shows the estimation error. The accuracy of the estimation was better than 7% for all layers.

## 4 EXPERIMENTAL FOR A FINGERTIP

### 4.1 MR Compression Test

We acquired MR volume data of index fingertips of one male subject with the age of 25. The finger nail of his right hand was glued to a cylindrical tube that is inserted into a small saddle coil placed at the center of a 4.7 T, 230 mm bore MRI scanner (Unity INOVA, Varian, Inc.). The high magnetic field of this scanner ensured high signal-to-noise ratio of the obtained data. The volume data was obtained with a three-dimensional gradient echo sequence (GE3D) with TR/TE of 20/10 msec, whose field of view (FOV) was  $120 \times 30 \times 30$  mm and volume size was  $512 \times 128 \times 128$  voxel. Reso-

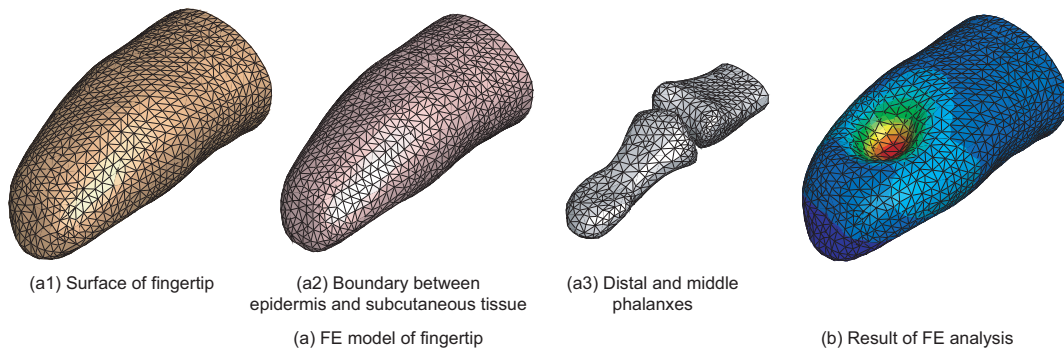


Figure 7: Generated finite element model of a fingertip and results of the finite element analysis.

lution of the volume data was thus  $234 \mu\text{m}/\text{voxel}$ . It took about 5 minutes to obtain a volume data.

A hydraulic compressor and an MR-compatible force sensor [9] were employed for this compression test. Both are highly MR-compatible: completely free from magnetic materials and electric circuits. We used hemispherical indent probe with the diameter of 5 mm. Center of the finger pad was indented in 5 steps. The maximum indentation depth was about 4 mm. Compression force was measured with the frequency of 1 Hz during the volume imaging process.

The following four preprocesses are applied to the volume data prior to iterative FE analysis: (1) trimming the volume data from the middle of the middle phalanx, (2) resizing the trimmed volume data to  $256 \times 128 \times 128$  so that the finger region is positioned at the center, (3) applying Gaussian filter of  $3 \times 3 \times 3$  voxel kernel to the resized volume data, and (4) normalizing the smoothed volume data so that the intensity values are scaled into the range of 0.0 to 1.0.

Figure 9 (a1) shows axial and sagittal slices of the compressed fingertip. One can observe multi-layered structures of soft tissue, phalanges and tendons in these figures. The cortical bright layer shows epidermis, while its interior that has slightly low intensity shows dermis. Innermost layer with irregular textures shows subcutaneous tissue. Observed compression force and its standard deviation are also shown in the top left of each sagittal slice.

Figure 6 shows the subtractions between the pre-compression sagittal slice and the measured sagittal slice at the final indentation step. The indenter made large deflections in the finger pad. At the same time, it makes a little deformation in the dorsal side of the fingertip. This makes the phalanges move upward in this slice. We can not, therefore, apply fixed boundary conditions to the phalanges.

## 4.2 FE model generation

Shape-morphing approach [16] was employed to generate subject-specific FE models. Different from the conventional approaches that generate individual FE model by applying segmentation and mesh generation to his/her medical volume data, this method generates individual FE model by applying spatial-morphing to a reference FE model without such time-consuming manual labors.

Spatial mapping that transform reference shape into target shape (in the case of this study, target is a fingertip of the subject) was computed by using volume registration for pre-compression MR volume data. See [16] for detail of this method and generation of a reference FE model. Shown in Figure 7 (a) is the generated FE model. This model has four anatomical parts, epidermis, subcutaneous tissue, distal phalanx and middle phalanx. This FE model consists of 35751 tetrahedral elements and 7006 nodes. Thickness

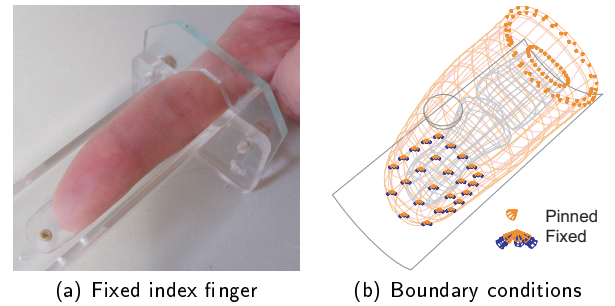


Figure 8: Index finger fixed on a cylindrical tube and boundary conditions applied to the FE model.

of the epidermis was about 0.6 mm that is almost consistent with the Dandekar's three-dimensional FE model [6].

Boundary conditions were assigned as follows. Nail region of the FE model was fixed, since the actual finger nail was glued to the cylindrical tube. A rigid element was generated to reproduce this cylindrical tube. Frictionless contact was assigned between this rigid element and dorsal side of the fingertip. End section of the finger model was pinned along the longitudinal direction. The indent probe was modeled by using discrete rigid element in which frictionless contact were assigned between the finger pad. Measured compression forces were applied to this indenter. Figure 8 (a) shows the actual index finger fixed on a cylindrical tube, while Figure 8 (b) shows the boundary conditions assigned to the FE model. Unlike similar analyses [4, 5, 6], we did not apply fixed or pinned condition to the phalanges because of the reason described in Section 4.1.

Material model of soft tissues was same as that assigned to the silicon rubber model in Section 3.2. Let us call the material constant of epidermis and subcutaneous tissue as  $\mu_{epi}$  and  $\mu_{sub}$ , respectively. Phalanges were assumed to be linear elastic and isotropic medium. The material constants were determined from the published data: Young's modulus was 10000 MPa and Poisson's ratio was 0.3. Figure 7 (b) shows the result of the FE analysis when  $\mu_{epi}$  was  $7.00\text{e-}2$  MPa and  $\mu_{sub}$  was  $7.00\text{e-}3$  MPa .

## 4.3 Iterative FE Analysis

The iterative FE analysis was conducted in two conditions. One is an estimation of material constant using homogeneous soft tissue (homogeneous model). In this case, epidermis and subcutaneous tissue were assumed to have the same material property, i.e.

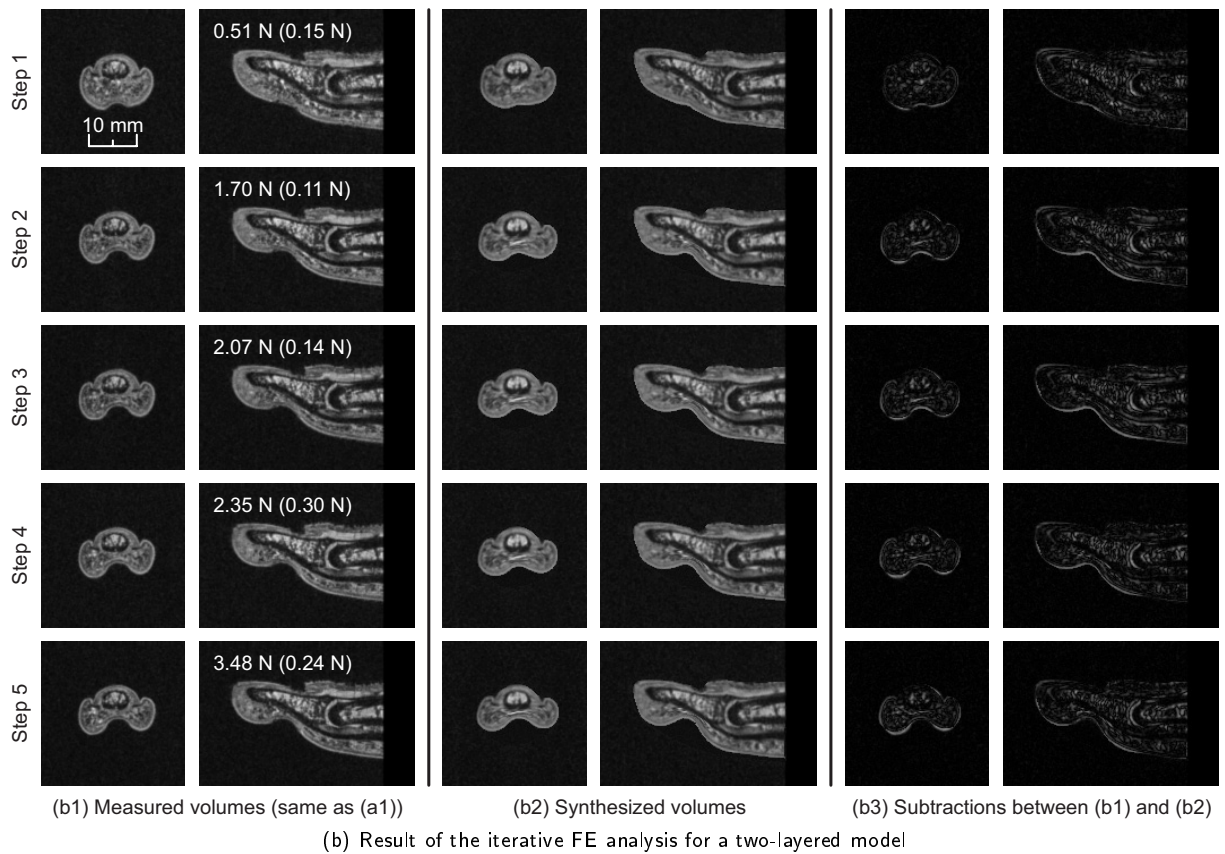
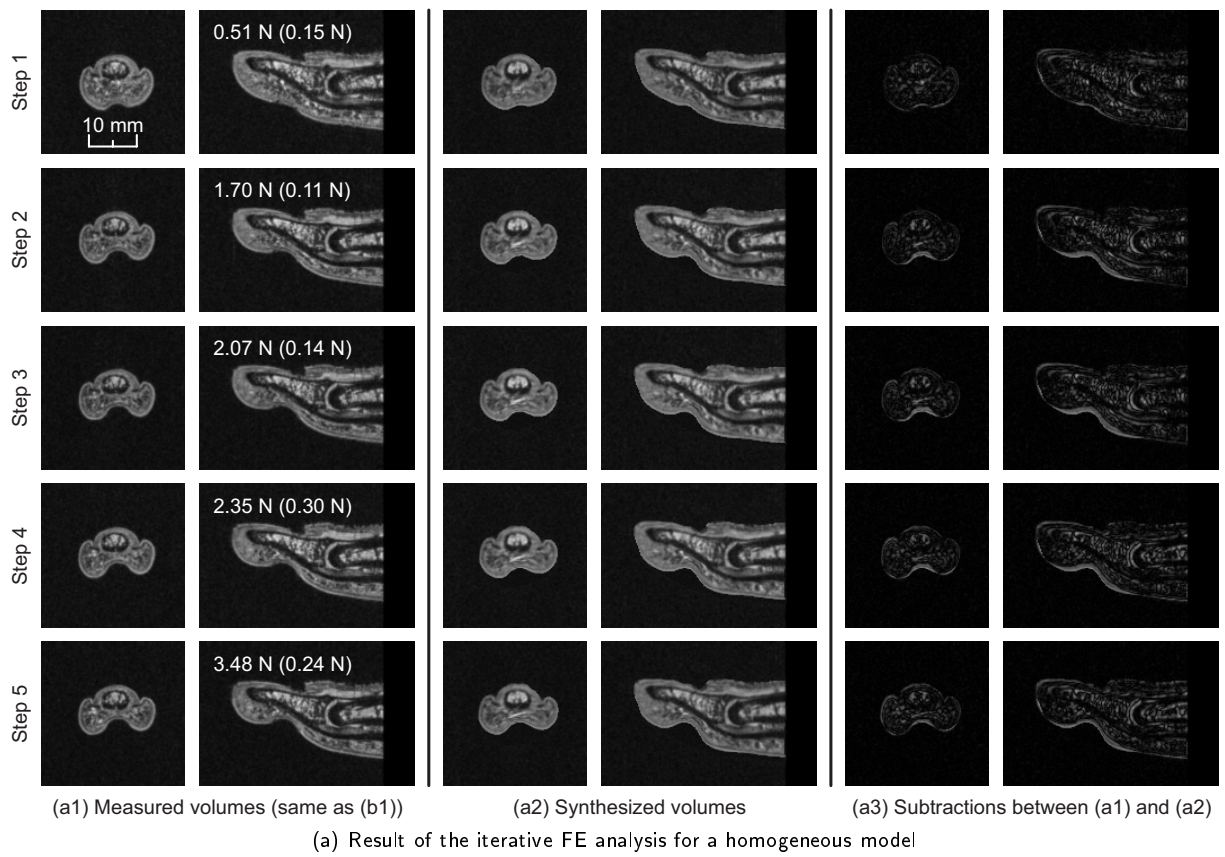


Figure 9: Measured volumes, warped volumes and subtractions between these volumes for different indentation depth.

Table 2: Initial material constants and estimated material constants for homogeneous model.

	$\mu_{epi} = \mu_{sub}$
Initial values (MPa)	1.00e-2
Estimated values (MPa)	2.31e-2

Table 3: Initial material constants and estimated material constants for two-layered model.

	$\mu_{epi}$	$\mu_{sub}$
Initial values (MPa)	7.00e-2	7.00e-3
Estimated values (MPa)	1.38e-1	7.98e-3

$\mu_{epi} = \mu_{sub}$ . It amounts to an optimization of one variable. The other is an estimation of material constants using layered soft tissue (layered model). In this case, epidermis and subcutaneous tissue were assumed to be independent, and, therefore, it is reduced to an optimization of two variables.

Several forward FE analyses were conducted in advance of the iterative FE analysis changing the material properties,  $\mu_{epi}$  and  $\mu_{sub}$ , systematically. The initial values of the optimization were determined from the material constants assigned in these pre-analyses such that the error between the measured volume and the synthesized volume is small enough. This helps to reduce necessary computational cost for the optimization. First rows of Table 2 and Table 3 show the initial value(s) in each analysis.

We chose to employ SSD as similarity measure of each optimization. The volumes captured in all steps were used to compute the SSD. We assigned 1.00e-3 MPa to  $tolx$  and 1.00e-3 to  $tolf$  in both optimizations as terminate criteria. Our current implementation requires approximately 2 hours (3 iterations) for the homogeneous model and 12 hours (8 iterations) for the layered model on a Pentium 4 3.8 GHz Windows machine with memory of 2 GB.

Figure 9 (a) shows the result of the iterative FE analysis for the homogeneous model. Each panel shows the measured volumes, synthesized volumes in the final iteration, and subtractions between these two volumes, respectively. Our optimization program succeeded to decrease the intensity error around the phalanges, while there is still much error in the surface shape. Figure 9 (b) shows the result of the iterative FE analysis for the layered model. Each panel shows the measured volumes, synthesized volumes in the final iteration, and subtractions between these two volumes, respectively. Our optimization program succeeded to decrease the intensity error of two volumes in total as compared to that for the homogeneous model. The layered model gives better estimation result that demonstrates that at least two-layered structure is necessary to conduct realistic FE analysis.

The second rows of Table 2 and Table 3 show the estimated material constants in each analysis. It should be noticed that epidermis is more rigid than the subcutaneous tissue that is consistent with material constants determined from a cadaver tissue [4]. The estimated material constants differ by an order of ten, that is consistent with Dandekar's result [6].

## 5 DISCUSSION

The results of the iterative FE analysis given in Section 4.3 have demonstrated essential characteristics of a fingertip: (1) it must have layered structure, and (2) the cortical layer is more rigid than the inner layer. These features are consistent with the previous

Table 4: Material constants identified/estimated in three works.

	$\mu_{epi}$	$\mu_{sub}$
Cadaver tissue [4] (MPa)	1.36e-1	0.34e-1
Simulation based method [6] (MPa)	1.80e-1	1.80e-2
Our method (MPa)	1.38e-1	7.98e-3

works [4, 6], although the value and ratio of elastic moduli differ as shown in Table 4. There are several reasons for this: difference in subject, estimation modality and material model. Then how we can validate the estimation results?

We believe that there are not true values in the material constants of living tissue. They must be, therefore, determined so that the estimated material constants fulfill certain criterion. In this research, similarity of two volumes measured by NMI or SSD was optimized for this purpose. In other word, material constants are determined such that the error between observed actual deformation and computed deformation is minimized. In that sense, the estimated material constants are valid and sufficient for our purpose, since we intend to conduct realistic FE analysis of individual three-dimensional fingertips.

Of course there are still much works to do to improve the quality of the estimation. As one can observe in Figure 9 (b3), there are still up to 0.5 mm differences in the axial slice images. In addition, material model is confined to an elastic one because of the limitation of imaging modality, although our method has potential to deal with visco-elastic properties.

In order to overcome such issues, we plan to develop new imaging modality capable of dynamic imaging, and to create more precise FE model that have real anatomical structure and necessary granularity of finite elements.

## 6 CONCLUSION

We have proposed a method to estimate material constants of living soft tissue. It allows modeling of non-linear material properties of soft tissue even for subsurface layer in non-invasive manner, since it employed medical imaging modality and iterative FE analysis. The iterative FE analysis determined material constants so that the error between measured MR volume data and synthesized MR volume data is minimized.

The proposed method was applied to a silicon rubber phantom and an index finger of male subject. The former result demonstrated the effectiveness of our method that estimated material constants with the accuracy of 7%. The latter result revealed an essential feature of a fingertip: the cortical layer is more rigid than the inner layer that is consistent with the previous researches.

This study has three future directions. First, we improve the quality of estimation by developing new imaging modality capable of dynamic imaging, and by creating more precise FE model that have real anatomical structure and necessary granularity of finite elements. Second, we apply presented method to hundred of people to figure out the variation of the material constants between individuals that will be much help for designer of industrial products dealt with hands. Finally, we conduct realistic FE analysis to investigate the mechanics of touch take the individual differences into consideration.

## REFERENCES

- [1] D. T. V. Pawluk and R. D. Howe. Dynamic lumped element response of the human fingerpad. *Journal of Biomechanical Engineering*, 121:178–183, 1999.

- [2] D. T. V. Pawluk and R. D. Howe. Dynamic contact of the human fingerpad against a flat surface. *Journal of Biomechanical Engineering*, 121:605–611, 1999.
- [3] N. Nakazawa, R. Ikeura, and H. Inooka. Characteristics of human fingertips in the shearing direction. *Biological Cybernetics*, 82:207–214, 2000.
- [4] T. Maeno, K. Kobayashi, and N. Yamazaki. Relationship between the structure of human finger tissue and the location of tactile receptor. *JSME International Journal*, 41:94–100, 1998.
- [5] J. Z. Wu, R. G. Dong, W. P. Smutz, and A. W. Schopper. Modeling of time-dependent force response of fingertip to dynamic loading. *Journal of Biomechanics*, 36:383–392, 2003.
- [6] K. Dandekar, B. I. Raju, and M. A. Srinivasan. 3-D finite-element models of human and monkey fingertips to investigate the mechanics of tactile sense. *Journal of Biomechanical Engineering*, 125:682–691, 2003.
- [7] R. Muthupillai, D. J. Lomas, P. J. Rossman, J. F. Greenleaf, A. Manduca, and R. L. Ehman. Magnetic resonance elastography by direct visualization of propagation acoustic strain waves. *Science*, 269:1854–1857, 1995.
- [8] T. L. Chenevert, A. R. Skovoroda, M. O'Donnell, and S. Y. Emelianov. Elasticity reconstructive imaging by means of stimulated echo MRI. *Journal of Magnetic Resonance in Medicine*, 39(3):382–490, 1998.
- [9] M. Tada and T. Kanade. Design of an MR-compatible three-axis force sensor. In *Proceedings of the IEEE/RSJ International Conference on Intelligent Robots and Systems (IROS)*, pages 2618–2623, 2005.
- [10] C. Studholme, D. Hill, and D. Hawkes. An overlap invariant entropy measure of 3D medical image alignment. *Pattern Recognition*, 32(1):71–86, 1999.
- [11] P. Anandan. A computational framework and an algorithm for the measurement of visual motion. *International Journal of Computer Vision*, 2(3):283–310, 1989.
- [12] J. C. Lagarias, J. A. Reeds, M. H. Wright, and P. E. Wright. Convergence property of the nelder-mead simplex method in low dimensions. *SIAM Journal of Optimization*, 9(1):112–147, 1998.
- [13] R. W. Ogden. Large deformation isotropic elasticity - on the correlation of the theory and experiment for incompressible rubberlike solids. *Proceedings of the Royal Society of London*, A.328:567–583, 1972.
- [14] O. H. Yeoh. On the ogden strain-energy function. *Rubber Chemistry and Technology*, 70:175–182, 1996.
- [15] M. Tada, N. Nagai, and T. Maeno. Material properties estimation of layered soft tissue based on MR observation and iterative FE simulation. In *Proceedings of the International Conference on Medical Image Computing and Computer Assisted Intervention (MICCAI)*, pages 633–640, 2005.
- [16] M. Tada, H. Yoshida, M. Mochimaru, and T. Kanade. Generating subject-specific FE models of fingertip with the use of MR volume registration. *to appear in Eurohaptics2006*.